



Available online at www.sciencedirect.com

ScienceDirect

journal homepage: <http://ees.elsevier.com/jot>



ORIGINAL ARTICLE

Biomechanical analysis of the camelid cervical intervertebral disc



Dean K. Stolworthy ^a, R. Amy Fullwood ^b, Tyler M. Merrell ^a,
Laura C. Bridgewater ^b, Anton E. Bowden ^{a,*}

^a Department of Mechanical Engineering, Brigham Young University, Provo, UT, USA

^b Department of Microbiology and Molecular Biology, Brigham Young University, Provo, UT, USA

Received 12 November 2014; accepted 3 December 2014

Available online 23 December 2014

KEYWORDS

alpaca;
animal model;
biomechanics;
camelid;
intervertebral disc

Summary Chronic low back pain (LBP) is a prevalent global problem, which is often correlated with degenerative disc disease. The development and use of good, relevant animal models of the spine may improve treatment options for this condition. While no animal model is capable of reproducing the exact biology, anatomy, and biomechanics of the human spine, the quality of a particular animal model increases with the number of shared characteristics that are relevant to the human condition. The purpose of this study was to investigate the camelid (specifically, alpaca and llama) cervical spine as a model of the human lumbar spine. Cervical spines were obtained from four alpacas and four llamas and individual segments were used for segmental flexibility/biomechanics and/or morphology/anatomy studies. Qualitative and quantitative data were compared for the alpaca and llama cervical spines, and human lumbar specimens in addition to other published large animal data. Results indicate that a camelid cervical intervertebral disc (IVD) closely approximates the human lumbar disc with regard to size, spinal posture, and biomechanical flexibility. Specifically, compared with the human lumbar disc, the alpaca and llama cervical disc size are approximately 62%, 83%, and 75% with regard to area, depth, and width, respectively, and the disc flexibility is approximately 133%, 173%, and 254%, with regard to range of motion (ROM) in axial-rotation, flexion-extension, and lateral-bending, respectively. These results, combined with the clinical report of disc degeneration in the llama lower cervical spine, suggest that the camelid cervical spine is potentially well suited for use as an animal model in biomechanical studies of the human lumbar spine.

Copyright © 2014, The Authors. Published by Elsevier (Singapore) Pte Ltd. This is an open access article under the CC BY-NC-ND license (<http://creativecommons.org/licenses/by-nc-nd/4.0/>).

* Corresponding author. Department of Mechanical Engineering, Brigham Young University, Provo, UT 84602, USA.
E-mail address: abowden@byu.edu (A.E. Bowden).

Introduction

Chronic low back pain (LBP) is a prevalent global problem, which is often correlated with degenerative disc disease. Available treatments for patients with chronic LBP have dismal satisfaction rates, and the development of novel treatments is hampered because we lack a testing model to effectively verify safety and efficacy.

Current *ex vivo* testing methodologies provide exceptionally useful information. For example, numerical analysis studies help analyse nutrient flow and mechanical flexibility; spine simulators may verify the numerical studies or provide benchmark comparison data for future devices; benchtop testing protocols using cadaver specimens increase our confidence in devices prior to FDA approval; and bioreactors allow testing cellular therapies. However, none of these models can demonstrate *in vivo* efficacy of treatments, thus the design/prototype/test cycle common to engineers is limited by the burdensome regulatory process required for human testing. In order to accelerate development of better treatments for LBP, a more readily accessible and characteristically similar model of the human condition is required [1,2].

Animals are an important part of biomedical research of the spine [1–4]. Each animal model has distinct advantages and disadvantages, yet no animal is capable of perfectly replicating the environment of the human spine, nor the degenerative condition of the human intervertebral disc (IVD), which has been linked with LBP. Age-related IVD degeneration is a virtually universal condition for humans yet remains largely absent from most of the animal kingdom. Only a few species are known to spontaneously degenerate: various canine breeds [5], ovine, and some primates (macaque monkeys and baboons) [6–8]. Of this group, only dogs have been reported to experience pain [5]. However, this pathology is limited to certain dog breeds that develop a condition called chondrodystrophy, which is genetically dissimilar from the typical course of disc degeneration observed in humans. Sheep have presented degeneration in their lumbar spine [9,10], but require further validation testing before wide acceptance. Also, while similarities may be drawn between the gravity load on the human spine and the muscle load on the quadruped spine, there remains much to learn about the effects of the differences in the biomechanical loading environment. Ethical concerns pre-emptively reduce our willingness to promote testing on primates [7,8,11–14].

Animal models of the spine have proven exceptionally useful in evaluating IVD mechanics and biomechanical changes due to induced disc degeneration [1,2,15]. However, there are fundamental differences in the biomechanical loading observed in the spine of most quadrupeds as compared with that of humans. Oriented resistance to gravity loading is a fundamental loading condition associated with erect posture and ambulation in humans, and most quadruped spines lack this characteristic, particularly in the lumbar spine. Many species of quadrupeds lack the range of motion (ROM) exhibited by human spines, particularly in axial rotation and flexion. Both humans and quadrupeds exhibit additional compressive loading due to

the intermediate and deep muscle loading and prestrain in passive stability elements (i.e., ligaments and fascia) of the spine, which varies by location [1,16], but the human lumbar spine exhibits a characteristic lordotic curvature that is in stark contrast to the kyphotic curvature in the lumbar region of quadrupeds. This difference in curvature contributes to a different loading condition and biomechanical motion profiles [17] for the IVD.

Painful degenerative disc disease was first documented in llamas in 2006 [18], and prompted our interest in investigating biomechanical and anatomical similarities between camelid and human spines, with the aim of determining the appropriateness of using camelids (specifically llamas and alpacas) as preclinical models for spine treatments. We aim to address key characteristics of a good animal model for the human IVD, including biomechanical flexibility testing, and disc morphology (shape and size) [18]. The purpose of this paper is to report on our findings for the camelid cervical IVD in the context of providing an animal model of the human lumbar IVD.

The camelid is skeletally mature by the age of 2 years and typically lives for 15–20 years. The spine consists of seven cervical vertebrae, 12 thoracic, seven lumbar, five sacral, and 11–17 caudal vertebrae. In general, the cervical vertebrae are relatively long compared to their transverse geometry, with the exception of the atlas (C1) and also the C7 vertebra, which is noticeably shorter than the other cervical vertebrae. The cervical vertebrae also have noticeable differences from the human lumbar vertebrae; specifically, the camelid vertebrae have two sets of lateral masses: cephalic and caudal protrusions extend ventrally to protect the blood vessels, trachea, and oesophagus. The vertebrae transverse-sectional geometry is smaller in the mid-transverse section and expands outward near the endplates. The cervical IVDs get larger with the lower segments, which is similar to the human lumbar spine. The facet joints of the camelid spine are similar in size to the human spine; however, the orientation is more vertical, and appears to act as a stabilizing guide during axial-rotation, rather than a hard-stop motion limiter during extension and/or lateral-bending motions, as seen in humans.

Materials and methods

Cervical spines were obtained from four alpacas and four llamas immediately following slaughter for purposes unrelated to this study. The spine specimens were further segmented into individual functional spinal units (FSUs) ranging from C2C3 to C7T1 for various studies, including flexibility/biomechanics, and morphology/anatomy. Each animal was young (2–4 years), but skeletally mature, and healthy with no known spinal disorders. Alpaca and llama test-specimens were obtained from a local, United States Department of Agriculture (USDA)-funded, camelid research center (The Camelid Center, Moroni, UT, USA). The center has a significantly larger population of alpacas as compared to llamas, thus these animals were more readily available and constitute the bulk of our testing specimens, and a limited number of llama specimens were also obtained for comparison based on availability.

Biomechanics and flexibility

Biomechanical flexibility tests were performed on 10 alpaca and three llama cervical segments, which were obtained from four alpacas: Alpaca1 (C3C4, C4C5, C5C6); Alpaca2 (C4C5, C6C7); Alpaca3 (C3C4, C4C5, C5C6); Alpaca4 (C4C5, C7T1); and a single llama: Llama1 (C2C3, C3C4, C5C6). Human samples used for statistical comparison were obtained from seven lumbar segments that were obtained from four human cadavers: Human1 (L1L2, L3L4, L5S1); Human2 (L1L2); Human3 (L2L3, L4L5); Human4 (L3L4) [19]. FSUs were cleansed of all extraneous muscle and adipose tissue and used for biomechanical flexibility testing. The passive nuchae ligament was also removed from each FSU due to attachment difficulties during biomechanical testing. Specimen preparation and testing followed published protocols [16,20,21]. Each specimen was sprayed with phosphate-buffered saline [22] at 5-minute intervals to maintain hydration during dissection and testing. Each FSU was potted using a two-part polyester resin (Bondo 265; 3M, St. Paul, MN, USA) [21] and secured in the test chamber, which maintained room temperature ($20 \pm 3^\circ\text{C}$).

Pure moment loads were applied in axial-rotation, flexion-extension, and lateral-bending, using a quasi-static, dynamic loading protocol with a continuous speed of 1 degree/s. A custom spine simulator [23,24] applied a symmetric ± 4 -newton meter (Nm) applied torque limit [25] in each loading direction to achieve the near-maximum segmental ROM without damaging any soft tissue. This torque limit was determined during exploratory flexibility studies on a single C6C7 cervical spinal segment: the sigmoidal torque-rotation curve approached the segmental limits of motion, where large changes in applied torque had little effect on the observed motion, and the torque-

rotation curve approached a horizontal asymptote (Fig. 1). This exploratory testing indicated that ± 4 Nm was a reasonable limit in all modal loading directions in the absence of a compressive follower load. Each FSU was preconditioned to this torque limit for a minimum of 20 cycles, when a repeatable torque-rotation response was observed. Multiple cycles of each testing condition were then recorded.

Data analysis

Segmental rotations in each of the primary modes of loading were computed from the 3D kinematic data. The sigmoidal torque-rotation response of each segment was centred about the ROM and fit with a pair of dual inflection point Boltzmann (DIP-Boltzmann) equations [23,24], which are of the form

$$\theta = \frac{ROM}{2} \cdot \left[1 - \frac{1}{1 + e^{\alpha_1(T-m_1)}} - \frac{1}{1 + e^{\alpha_2(T-m_2)}} \right].$$

The dependent variable, θ , represents the overall rotation of the upper vertebra with respect to the lower vertebra. ROM is the segmental range of motion, T is the applied torque (independent variable), m_1 and m_2 identify the location of the inflection points, and α_1 and α_2 are associated with the growth rate near m_1 and m_2 . The full nonlinear, viscoelastic response of the segment was captured using the two DIP-Boltzmann equations to model the torque-rotation response (1 upper, 1 lower: unloading \rightarrow loading, with an average coefficient of determination of 99%) for each test, as well as to easily calculate several FSU flexibility parameters [ROM, neutral zone (NZ), hysteresis (H), and neutral-zone stiffness (K)], which

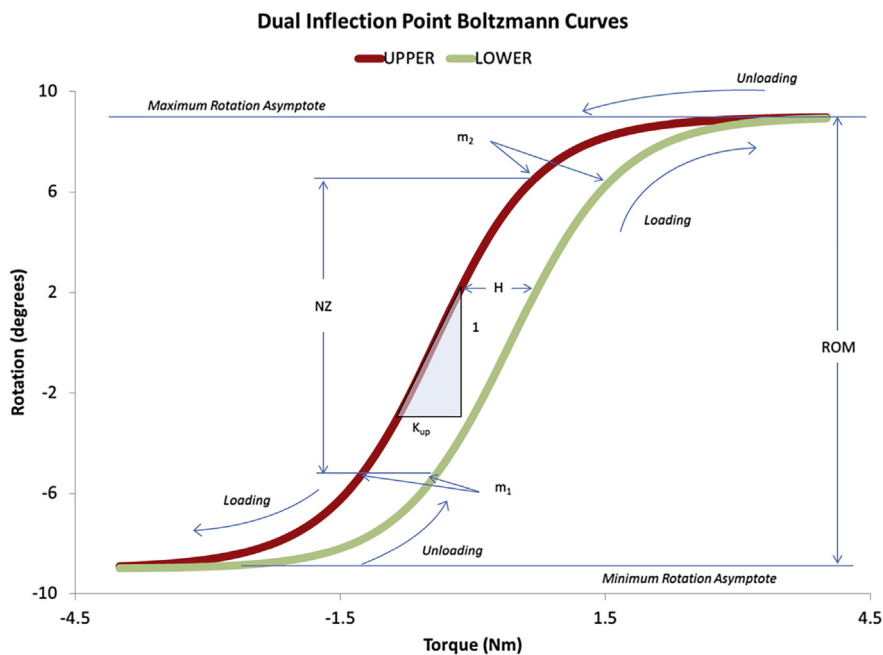


Figure 1 Two DIP-Boltzmann curves (1 upper, 1 lower) are fit to the experimental data to characterize the flexibility of the FSU, according to the flexibility parameters shown (ROM, NZ, K_{NZ} , H). DIP = dual inflection point; H = hysteresis; K_{NZ} = neutral zone stiffness; NZ = neutral zone; ROM = range of motion.

describe the viscoelastic torque-rotation according to [23,24] (Fig. 1). These flexibility parameters were calculated numerically in order to reduce subjective results. ROM is the maximum distance between the upper and lower asymptotes; NZ is defined as the portion of the torque-rotation curve where lots of motion occurs with little torque input. NZ was calculated as the maximum vertical distance between the upper and lower curves; H is calculated numerically as the average horizontal spread between the upper and lower curve within the NZ; and K is calculated as the average stiffness within the NZ. For further explanation of the flexibility parameters, please refer to [23,24].

Collected data was analysed using a mixed model analysis of variance (ANOVA) test corresponding to loading direction (axial-rotation, flexion-extension, and lateral-bending), species (alpaca, llama, human), and blocking on the randomized test specimen. Human lumbar data used for statistical comparison was obtained from published test data using the same testing protocols and spine tester, according to [19,24], and the human data used was limited to healthy IVDs (Thompson grade degeneration less than 2) that came from published data on seven human lumbar IVDs [19]. Descriptive statistics [mean and standard deviation (SD)] were calculated for the observed/calculated flexibility parameters, and are presented for comparison between species.

Disc morphology

Morphological studies were performed on 17 alpaca IVDs and nine llama IVDs, which were obtained from four alpacas: Alpaca1 (C3C4, C4C5, C5C6, C6C7); Alpaca2 (C2C3, C6C7); Alpaca3 (C2C3, C4C5, C5C6, C6C7, C7T1); Alpaca4 (C2C3, C3C4, C4C5, C5C6, C7T1); and three llamas: Llama1 (C2C3, C5C6); Llama2 (C2C3, C3C4, C4C5, C5C6); Llama3 (C2C3, C3C4, C4C5). Cervical segments were transected and imaged to compare disc morphology, including the disc shape and size. The disc shape was observed in the transverse and sagittal planes, with the focus on the curvature of the cephalic and caudal endplates of the disc. The disc size was measured using calibrated optical photogrammetry of the mid-transverse and mid-sagittal sections of the disc using MATLAB® Image Processing Toolbox (MathWorks Inc., Natick, MA, USA) to quantify the size (Fig. 2). Three researchers with experience in IVD anatomy each made three measurements of the disc dimensions from the images. Analysis of these measurements showed no significant difference ($p < 0.05$) between observations (intra-observer reliability) or researchers (inter-observer reliability) using a mixed model analysis. Reported results represent an average of all the measurements taken and a pooled standard deviation (SD). Whole disc (WD) anterior–posterior (AP) width was measured as the maximum straight-line distance from the middle anterior to the middle posterior annular region, including the annular and nuclear regions (Fig. 2). WD lateral width was measured as the maximum straight-line distance from the middle left lateral to the middle right lateral region, which also included the annular and nuclear regions. Nucleus pulposus (NP) AP width was measured as the maximum straight-line distance from the

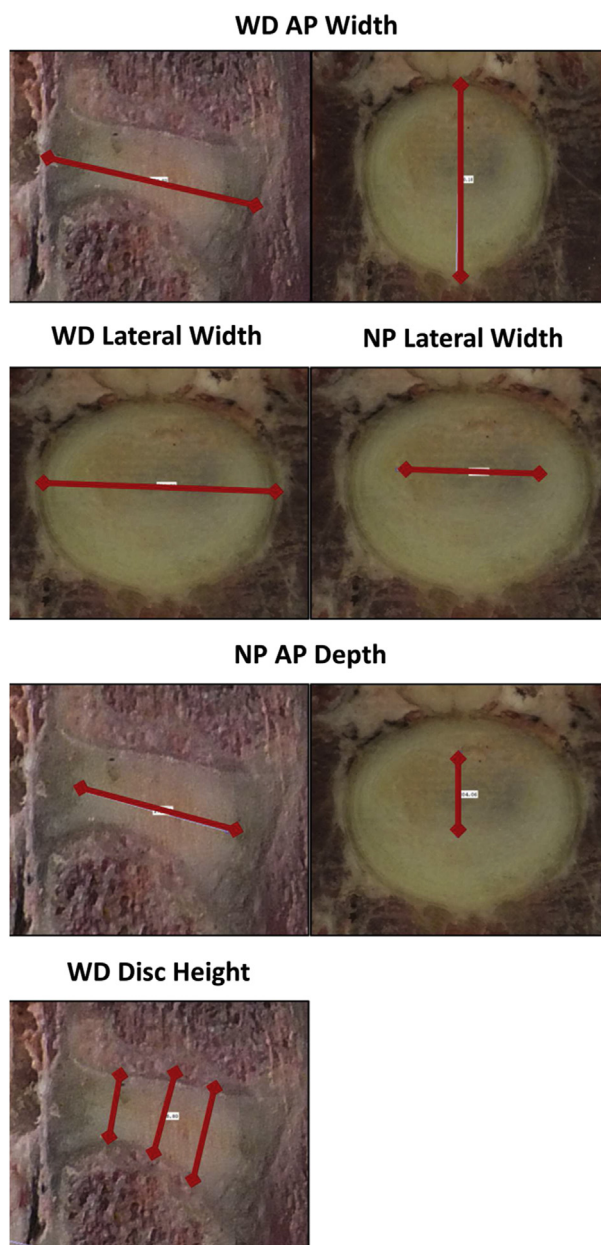


Figure 2 Measurement procedure of the sections of the camelid (alpaca and llama) cervical IVD. AP = anterior posterior; IVD = intervertebral disc; NP = nucleus pulposus; WD = whole disc.

middle anterior to the middle posterior nuclear region, not including the inner annulus. NP lateral width was measured as the maximum straight-line distance from the middle left lateral to the middle right lateral annular region, not including the inner annulus. Annulus fibrosus (AF) AP width was calculated as the difference between the whole disc AP width and the NP AP width. AF lateral width was calculated as the difference between the whole disc lateral width and the NP lateral width. Disc height was estimated as the average distance between the cranial and caudal endplates within the bounds of the NP. Disc shape was evaluated in the mid-sagittal section according to the concavity of the cephalic and caudal endplates, and mid-transverse sections

according to the elliptical axes, which are captured by the AP width and lateral width.

Results

Postural similarities

Alpacas and llamas present four anatomical characteristics that enforce a similar biomechanical loading condition in their cervical spine to that experienced in the human lumbar spine: (1) their natural posture aligns the loading of their cervical vertebrae vertically to resist gravity loading in an open kinetic chain; (2) the gravity load supported by the lower portion of the spine is magnified due to the extended length of the neck; (3) the cervical vertebrae exhibit a lordotic curvature similar to that of the human lumbar spine; and (4) the lordotic curvature presents itself secondary to weight bearing in the upright position, whereas the primary (embryotic) curvature is kyphotic.

Biomechanics and flexibility

Segmental biomechanics and flexibility parameters in the three primary modes of loading were captured through the torque-rotation response that exhibited the expected sigmoidal shape (Fig. 3, Table 1) that is consistent with human spine biomechanics [23,24]. Flexibility parameters of ROM, NZ, K, and H, were determined from the torque-rotation curves and are shown with published human lumbar and cervical parameters. Boxplots of the ROM and other flexibility parameters (NZ, K_{NZ} , and H) for the alpaca and llama (Fig. 4) [19,24,26–28] appear nearly identical, with no significant difference (Table 2) found for any of the flexibility parameters (ROM, NZ, H, K) between alpacas and llamas. In axial rotation, the camelid ROM was nearly identical with the human lumbar spine. In flexion-extension and lateral-bending, however, the camelid segments were significantly more flexible than the human lumbar spine ($p < 0.01$) and closer to data reported for the human cervical spine [26]. Regardless, multiple similarities with the human spine were observed with NZ, H, and K (Fig. 4). Significance levels for the various flexibility parameters and their differences across species can be found in Table 2.

Table 1 Flexibility parameters (ROM, NZ, K_{NZ} , H) of the alpaca and llama cervical spine segments.

Species	Dir	N	Statistic	ROM	NZ	K_{NZ}	H
Alpaca	AR	10	Mean	4.6	0.9	1.5	1.1
			SD	2.1	0.3	0.8	0.4
			Min	2.2	0.5	0.5	0.6
			Max	8.7	1.6	2.8	1.8
	FE	7	Mean	25	2.9	0.2	0.5
			SD	2.3	0.3	0	0.1
			Min	21.4	2.3	0.1	0.4
	LB	9	Mean	28.4	4	0.2	0.6
			SD	7.4	2	0.1	0.2
Min			13.3	1.8	0.1	0.4	
Llama	AR	3	Mean	6	1	0.9	0.9
			SD	1.3	0.2	0.3	0.1
			Min	4.5	0.8	0.7	0.9
			Max	7.1	1.2	1.2	1
	FE	3	Mean	27.3	3.2	0.2	0.5
			SD	3.3	0.4	0	0.1
			Min	23.6	2.8	0.1	0.4
	LB	3	Mean	32.8	5.4	0.1	0.7
			SD	2.8	1.9	0	0.2
Min			29.7	3.8	0.1	0.5	
			Max	35	7.5	0.2	1

AR = axial-rotation; Dir = direction; FE = flexion-extension; H = hysteresis; K_{NZ} = neutral-zone stiffness; LB = lateral-bending; NZ = neutral zone; ROM = range of motion.

Available flexibility data in published literature was mostly limited to ROM, with some also reporting NZ. When comparing the ROM of alpaca, llama, and other large animal models used for human lumbar spine biomechanics testing, the llama and alpaca presented the expected results that they had a comparable ROM as the human lumbar spine or the other large animal models (Fig. 5) [15,19, 21, 26,29–33]. The increased ROM observed in flexion-extension and lateral-bending was expected due to the removal of the large nuchal ligament from the posterior spine, thereby greatly decreasing the passive stiffness of the segment.

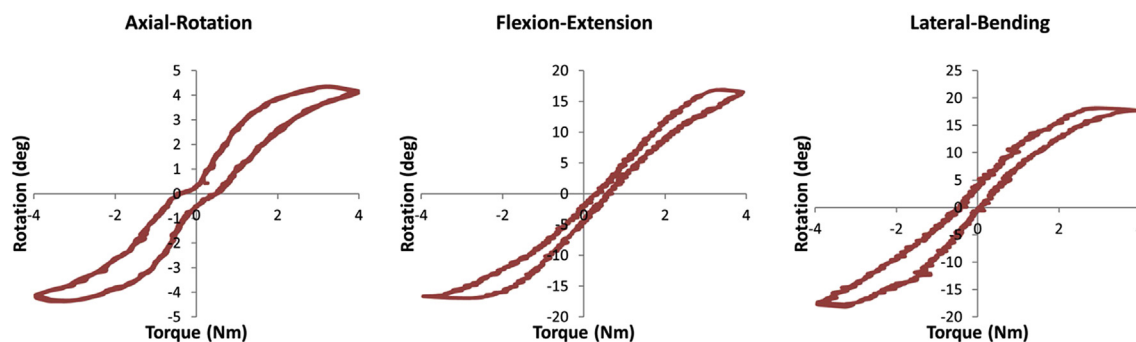


Figure 3 Flexibility tests captured the torque-rotation response of alpacas and llamas in the three modal axes of loading: axial-rotation (left), flexion-extension (middle), and lateral-bending (right).

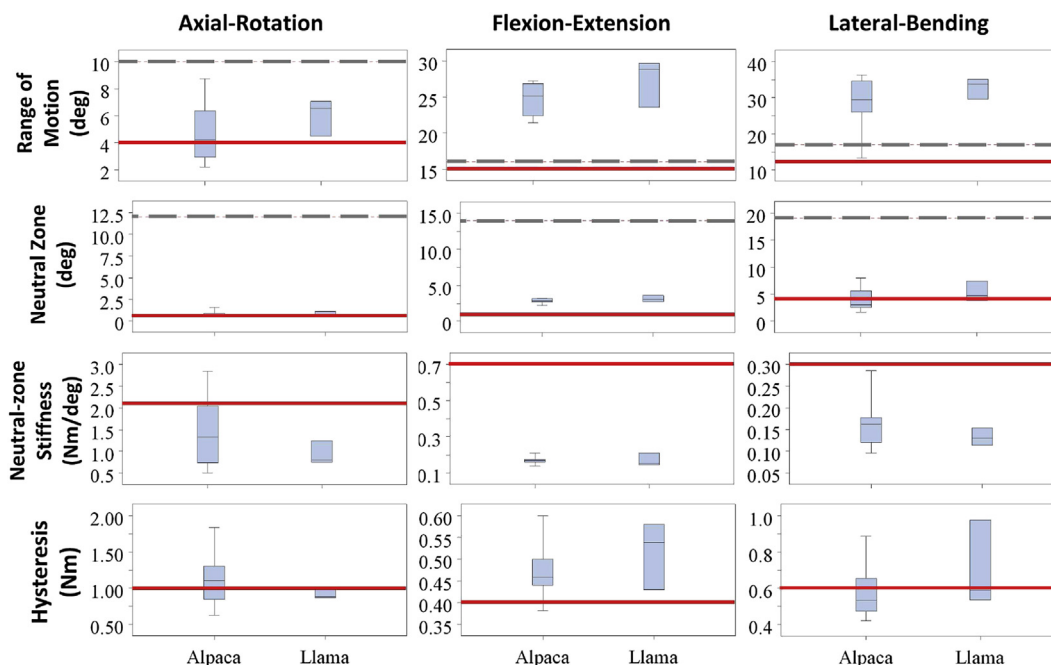


Figure 4 Flexibility parameters of the alpaca and llama cervical spine shown with reference to comparable values for the human lumbar (—) [19,24,26] and human cervical (---, not shown for neutral-zone stiffness and hysteresis) [26–28] spine.

Table 2 Significance levels for how the species affects the biomechanical flexibility parameters (ROM, NZ, K_{NZ} , H).

Species	Significance levels (<i>p</i>)			
	ROM	NZ	H	K_{NZ}
Human lumbar vs. alpaca	<0.005	0.28	0.48	0.09
Human lumbar vs. llama	<0.005	0.14	0.70	0.08
Alpaca vs. llama	0.18	0.25	0.81	0.29

H = hysteresis; K_{NZ} = neutral-zone stiffness; NZ = neutral zone; ROM = range of motion.

Disc morphology and size

Original data for the alpaca and llama cervical IVDs is presented to compare against currently published large animal models. The size of the alpaca and llama cervical IVDs more closely approach the size of the human lumbar IVD than current large animal models, particularly with regard to the total, NP, and AF AP width, as well as the AF lateral width and disc height (Fig. 6 [26,34–40], Table 3). Published size data of current large animal IVDs is presented with comparison to the human lumbar IVD (as represented by the horizontal reference line). A benefit of an animal model with comparable disc size is that mechanical loading is challenging to normalize based on geometric parameters. A familiar example is that pressure is a normalization of the force by the cross-sectional area. However, comparison of applied moment conditions, or the more physiologic applied moment plus compressive follower load conditions, are challenging to normalize, thus direct comparison of discs that have similar size holds tremendous appeal.

The alpaca and llama discs proved to be similar in size with each other. The alpaca disc anatomy was generally smaller except for the AF, which was surprisingly thicker in both the AP depth and the lateral width (Figs. 6 and 7, Table 2). The shape of the disc in the mid-transverse plane appeared elliptical, with no deviations in the posterior-lateral regions. Thus, by capturing the disc AP and lateral width, the elliptical shape can be accurately captured. In the mid-sagittal section, alpaca and llama cervical discs are approximately planar on the cephalic endplate and concave on the caudal endplate.

Discussion

Published reports of painful disc bulging and herniation in a middle-aged llama [18] prompted the authors’ theory that the camelid cervical IVD would make a good animal model of the human lumbar IVD, and the present work showed substantial similarities with regard to spinal posture, biomechanics, and IVD size. These shared characteristics present a unique model with potential for testing various physical, cellular, or surgical treatments, which may be more rapidly translated to viable treatments for LBP in humans.

The camelid cervical segments appeared to be more flexible than the human lumbar segments in flexion-extension and lateral-bending; however, this increased flexibility may be attributed to the methodological procedure of removing the bilateral nuchal ligaments, which are assumed to significantly increase the stiffness and resistance to the flexion and lateral-bending motions. However, this increased ROM may also be attributed to the different orientation of the facets. Preserving all ligaments for future *ex vivo* studies is encouraged, and *in vivo* uses of a camelid

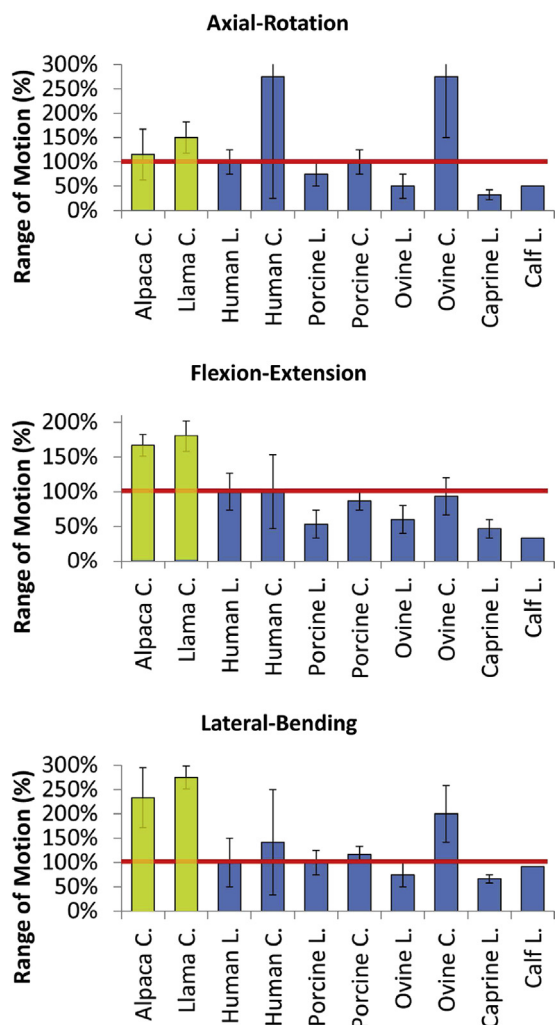


Figure 5 Approximate range of motion (ROM) of several large animal spine segments (C = cervical; L = Lumbar) in axial-rotation, flexion-extension, and lateral-bending as a percentage of human lumbar ROM [15,26,29–31], which is represented as the horizontal reference line. References for provided benchmark data are as follows: Human L. [19,21,26,32], Human C. [33], Porcine L. and Porcine C. [29], Ovine L. and Ovine C. [31], Caprine L. [15], Calf L [30].

spine model with intact nuchal ligaments may yield flexion-extension and lateral-bending motions that are more consistent with the human lumbar spine and could determine whether the facets' orientation significantly affect the range of motion. As the authors expected, with llamas being taller and heavier, their cervical spine segments were slightly larger in size than the alpaca segments, however the effects on biomechanical motion did not show any statistical significance. The limited number of available llama specimens used may have limited the statistical resolution of this study.

A consequence of IVD size discrepancy concerns the applicability of human-sized spinal interventions. Preclinical animal models of the spine are regularly used to investigate safety and efficacy of spinal fusion hardware [4], scoliosis instrumentation [41], artificial spinal discs [15,42], etc. Thus, size incongruity of the disc limits

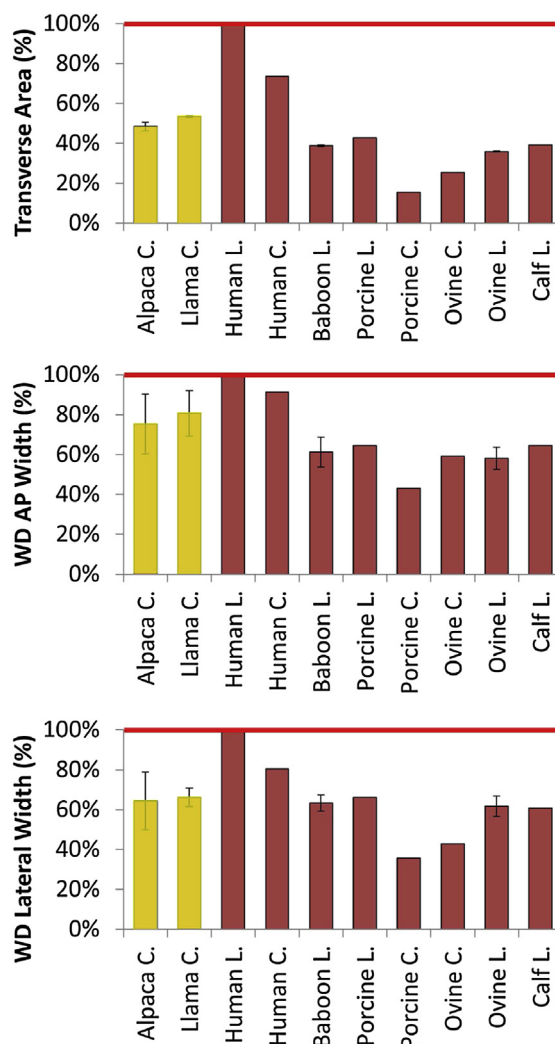


Figure 6 Approximate IVD size (area, depth, width) comparison between camelid (alpaca and llama) and large animal spine segments (C = cervical; L = lumbar) from published literature [34–38], as a percentage of the respective human lumbar dimension [26,34,36,39,40], which is represented with the horizontal reference line. SDs are shown where available. AP = anterior posterior; IVD = intervertebral disc; SD = standard deviation.

applicability of observed efficacy data from these preclinical animal studies. As a consequence, preclinical animal testing of spinal instrumentation is often viewed as an extended biocompatibility test, rather than providing valid functional data. Our results demonstrate that llama and alpaca discs are significantly closer in size to human discs than other animal models, and thus have potential to provide a more direct comparison of disc repair and regeneration treatments.

Human lumbar discs are wedge-shaped with endplate convexity on both the cephalic and caudal endplates, when viewed from the sagittal or frontal planes [1]. This convexity provides biomechanical benefits in terms of increased stability and contact area and induces an asymmetric flexion-extension kinematic response. It also results in an increased transport distance (and therefore difficulty)

Table 3 Alpaca and llama cervical IVD size comparison with the human lumbar IVD.

Measured in mm		Alpaca cervical		Llama cervical		Human lumbar	
		N	Mean (SD)	N	Mean (SD)	Mean (SD)	Source
Whole disc	Height	5	8.3 (0.56)	2	8.8 (0.94)	8.1 (1.7)	[2]
	AP width					11.3 (0.3)	[36]
						34.4 (1.1)	[1]
						35.8 (1.7)	[2]
Lateral width					37.2 (4.7)	[36]	
					47.1 (1.2)	[1]	
					49.0 (3.7)	[2]	
					55.9 (9.4)	[36]	
Nucleus pulposus	AP width	16	11.1 (2.67)	8	14.6 (3.26)	20.8 (2.0)	[36]
	Lateral width	11	16.0 (4.32)	5	20.2 (3.31)	27.3 (3.2)	[36]
Annulus fibrosus	AP width	16	17.0 (4.29)	8	15.7 (3.72)	16.4 (3.6)	[36]
	Lateral width	11	20.3 (6.46)	5	17.1 (2.40)	28.6 (7.0)	[36]

AP = anterior–posterior; IVD = intervertebral disc; SD = standard deviation.

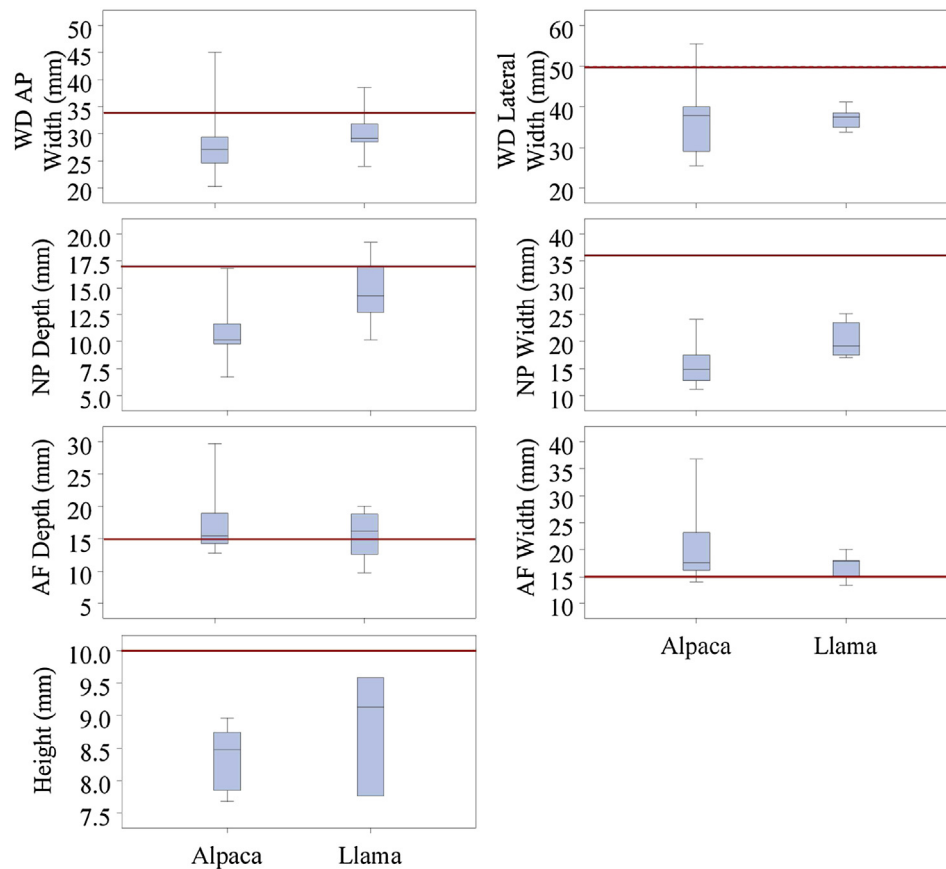


Figure 7 Alpaca (left box) and llama (right box) cervical intervertebral disc (IVD) size comparison with the human lumbar IVD (reference line shown as average of human data in [Table 2](#)).

for nutrient and waste exchange with the vasculature in the adjacent vertebrae. While the transverse planar shape of the human disc is sometimes approximated as an ellipse, it actually exhibits a more convoluted (e.g., “lima bean”) shape ([Fig. 8](#)) due to accommodation of the spinal canal along the posterior aspect. This unique shape creates stress concentration points in the posteriolateral regions of the

disc during lumbar extension. This portion of the disc also coincides with the primary location of radial fissures and nuclear protrusions [[9,10](#)]. Llama and alpaca cervical discs are significantly different in shape from human lumbar discs, exhibiting a roughly ellipsoid shape, although they do exhibit the same wedge shape as viewed from the sagittal plane.

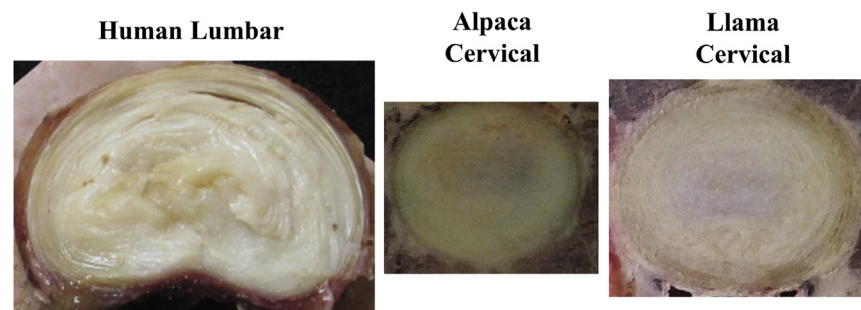


Figure 8 Relative intervertebral disc (IVD) size/shape comparison of the human lumbar (left), alpaca cervical (middle), and llama cervical (right); a consistent scale was maintained across the images.

In summary, the authors believe the results provided in the present work show that a camelid IVD model sufficiently mimics the human lumbar IVD with regard to spinal posture, size, shape, and biomechanics. The classification of spontaneous disc degeneration in the cervical spine is consistent with a lack of notochord cells, which is common with large animals. Future work may involve regeneration studies of a spontaneously degenerated IVD, which has been limited in the past by the availability of a viable large animal model, and further testing and validation is needed to better understand the application of this work in regards to the camelid's susceptibility to IVD degeneration and the potential for regeneration. Regardless, as alpaca or llama farms are located throughout the world (including over 1800 registered alpaca farms located throughout all regions of the US), the results presented here indicate exciting potential for using camelids as a model of human lumbar disc degeneration.

Conflicts of interest

All authors declare no conflicts of interest.

Acknowledgements

Special thanks to Dr Todd Robinson of the Camelid Center for providing the alpaca test specimens. Research funding for this work was provided by Brigham Young University.

References

- [1] Alini M, Eisenstein SM, Ito K, Little C, Kettler AA, Masuda K, et al. Are animal models useful for studying human disc disorders/degeneration? *Eur Spine J* 2008;17:2–19.
- [2] Lotz JC. Animal models of intervertebral disc degeneration: lessons learned. *Spine (Phila Pa 1976)* 2004;29:2742–50.
- [3] Showalter BL, Beckstein JC, Martin JT, Beattie EE, Espinoza Orias AA, Schaer TP, et al. Comparison of animal discs used in disc research to human lumbar disc: torsion mechanics and collagen content. *Spine (Phila Pa 1976)* 2012;37:E900–7.
- [4] Drespe IH, Polzhofer GK, Turner AS, Grauer JN. Animal models for spinal fusion. *Spine J* 2005;5:2095–2016S.
- [5] Bergknut N, Rutges JP, Kranenburg HJ, Smolders LA, Hagman R, Smidt HJ, et al. The dog as an animal model for intervertebral disc degeneration? *Spine (Phila Pa 1976)* 2012;37:351–8.
- [6] Lauerman WC, Platenberg RC, Cain JE, Deeney VF. Age-related disk degeneration: preliminary report of a naturally occurring baboon model. *J Spinal Disord* 1992;5:170–4.
- [7] Nuckley DJ, Kramer PA, Del Rosario A, Fabro N, Baran S, Ching RP. Intervertebral disc degeneration in a naturally occurring primate model: radiographic and biomechanical evidence. *J Orthop Res* 2008;26:1283–8.
- [8] Kramer PA, Newell-Morris LL, Simkin PA. Spinal degenerative disk disease (DDD) in female macaque monkeys: epidemiology and comparison with women. *J Orthop Res* 2002;20:399–408.
- [9] Baker JR, Lyon DG. A case of intervertebral disc degeneration and prolapse with spondylosis in a sheep. *Vet Rec* 1975;96:290.
- [10] Reid JE, Meakin JR, Robins SP, Skakle JM, Hukins DW. Sheep lumbar intervertebral discs as models for human discs. *Clin Biomech* 2002;17:312–4.
- [11] Cunningham BW, Berven SH, Hu N, Beatson HJ, De Deyne PG, McAfee PC. Regeneration of a spinal ligament after total lumbar disk arthroplasty in primates. *Cells Tissues Organs* 2009;190:347–55.
- [12] Elias PZ, Nuckley DJ, Ching RP. Effect of loading rate on the compressive mechanics of the immature baboon cervical spine. *J Biomech Eng* 2006;128:18–23.
- [13] Tominaga T, Dickman CA, Sonntag VK, Coons S. Comparative anatomy of the baboon and the human cervical spine. *Spine (Phila Pa 1976)* 1995;20:131–7.
- [14] Gal J. Mammalian spinal biomechanics: postural support in seated macaques. *J Exp Biol* 2002;205:1703–7.
- [15] Detiger SE, Hoogendoorn RJ, van der Veen AJ, van Royen BJ, Helder MN, Koenderink GH, et al. Biomechanical and rheological characterization of mild intervertebral disc degeneration in a large animal model. *J Orthop Res* 2013;31:703–9.
- [16] Patwardhan AG, Havey RM, Carandang G, Simonds J, Voronov LI, Ghanayem AJ, et al. Effect of compressive follower preload on the flexion-extension response of the human lumbar spine. *J Orthop Res* 2003;21:540–6.
- [17] Bertram JE, Gutmann A. Motions of the running horse and cheetah revisited: fundamental mechanics of the transverse and rotary gallop. *J R Soc Interface* 2009;6:549–59.
- [18] Valentine BA, Saulez MN, Cebra CK, Fischer KA. Compressive myelopathy due to intervertebral disk extrusion in a llama (*Lama glama*). *J Vet Diagn Invest* 2006;18:126–9.
- [19] Stolworthy DK. Characterization and biomechanical analysis of the human lumbar spine with *in vitro* testing conditions (Thesis). Brigham Young University; 2012.
- [20] Hongo M, Gay RE, Hsu JT, Zhao KD, Ilharreborde B, Berglund LJ, et al. Effect of multiple freeze-thaw cycles on intervertebral dynamic motion characteristics in the porcine lumbar spine. *J Biomech* 2008;41:916–20.
- [21] Panjabi MM, Oxland TR, Yamamoto I, Crisco JJ. Mechanical behavior of the human lumbar and lumbosacral spine as shown

- by three-dimensional load-displacement curves. *J Bone Jt Surg Am* 1994;76:413–24.
- [22] Busscher I, van der Veen AJ, van Dieen JH, Kingma I, Verkerke GJ, Veldhuizen AG. *In vitro* biomechanical characteristics of the spine: a comparison between human and porcine spinal segments. *Spine (Phila Pa 1976)* 2010;35:E35–42.
- [23] Stolworthy DK, Zirbel SA, Howell LL, Samuels M, Bowden AE. Characterization and prediction of rate-dependent flexibility in lumbar spine biomechanics at room and body temperature. *Spine J* 2014;14:789–98.
- [24] Zirbel SA, Stolworthy DK, Howell LL, Bowden AE. Intervertebral disc degeneration alters lumbar spine segmental stiffness in all modes of loading under a compressive follower load. *Spine J* 2013;13:1134–47.
- [25] Acosta FL, Buckley JM, Xu Z, Lotz JC, Ames CP. Biomechanical comparison of three fixation techniques for unstable thoracolumbar burst fractures. *J Neurosurg Spine* 2008;8:341–6.
- [26] White AA, Panjabi MM. *Clinical biomechanics of the spine*. Philadelphia: Lippincott; 1990.
- [27] Panjabi MM, Crisco JJ, Vasavada A, Oda T, Cholewicki J, Nibu K, et al. Mechanical properties of the human cervical spine as shown by three-dimensional load-displacement curves. *Spine (Phila Pa 1976)* 2001;26:2692–700.
- [28] Panjabi MM, Summers DJ, Pelker RR, Videman T, Friedlaender GE, Southwick WO. Three-dimensional load-displacement curves due to forces on the cervical spine. *J Orthop Res* 1986;4:152–61.
- [29] Wilke HJ, Geppert J, Kienle A. Biomechanical *in vitro* evaluation of the complete porcine spine in comparison with data of the human spine. *Eur Spine J* 2011;20:1859–68.
- [30] Kettler A, Liakos L, Haegele B, Wilke HJ. Are the spines of calf, pig and sheep suitable models for pre-clinical implant tests? *Eur Spine J* 2007;16:2186–92.
- [31] Wilke HJ, Kettler A, Claes LE. Are sheep spines a valid biomechanical model for human spines? *Spine (Phila Pa 1976)* 1997;22:2365–74.
- [32] Yamamoto I, Panjabi MM, Crisco T, Oxland T. Three-dimensional movements of the whole lumbar spine and lumbosacral joint. *Spine (Phila Pa 1976)* 1989;14:1256–60.
- [33] Wen N, Lavaste F, Santin JJ, Lassau JP. Three-dimensional biomechanical properties of the human cervical spine *in vitro*. I. Analysis of normal motion. *Eur Spine J* 1993;2:2–11.
- [34] Schmidt H, Reitmaier S. Is the ovine intervertebral disc a small human one? A finite element model study. *J Mechan Behav Biomed Mater* 2013;17:229–41.
- [35] Sheng SR, Wang XY, Xu HZ, Zhu GQ, Zhou YF. Anatomy of large animal spines and its comparison to the human spine: a systematic review. *Eur Spine J* 2010;19:46–56.
- [36] Busscher I, Ploegmakers JJ, Verkerke GJ, Veldhuizen AG. Comparative anatomical dimensions of the complete human and porcine spine. *Eur Spine J* 2010;19:1104–14.
- [37] Beckstein JC, Sen S, Schaer TP, Vresilovic EJ, Elliott DM. Comparison of animal discs used in disc research to human lumbar disc: axial compression mechanics and glycosaminoglycan content. *Spine (Phila Pa 1976)* 2008;33:E166–73.
- [38] O’Connell GD, Vresilovic EJ, Elliott DM. Comparison of animals used in disc research to human lumbar disc geometry. *Spine (Phila Pa 1976)* 2007;32:328–33.
- [39] Cannella M, Arthur A, Allen S, Keane M, Joshi A, Vresilovic E, et al. The role of the nucleus pulposus in neutral zone human lumbar intervertebral disc mechanics. *J Biomech* 2008;41:2104–11.
- [40] Panjabi MM, Goel V, Oxland T, Takata K, Duranceau J, Krag M, et al. Human lumbar vertebrae. Quantitative three-dimensional anatomy. *Spine (Phila Pa 1976)* 1992;17:299–306.
- [41] Odent T, Cachon T, Peultier B, Gournay J, Jolivet E, Elie C, et al. Porcine model of early onset scoliosis based on animal growth created with posterior mini-invasive spinal offset tethering: a preliminary report. *Eur Spine J* 2011;20:1869–76.
- [42] Halverson PA, Bowden AE, Howell LL. A compliant-mechanism approach to achieving specific quality of motion in a lumbar total disc replacement. *Int J Spine Surg* 2012;6:78–86.